ERDC/CHL TR-04-10

US Army Corps
of Engineers®
Engineer Research and
Development Center

Multidimensional Numerical Modeling of Surges Over Initially Dry Land

R. C. Berger and L. M. Lee

September 2004

Coastal and Hydraulics Laboratory

ERDC/CHL TR-04-10
September 2004

Multidimensional Numerical Modeling of Surges Over Initially Dry Land

R. C. Berger and L. M. Lee

Coastal and Hydraulics Laboratory
U.S. Army Engineer Research and Development Center
3909 Halls Ferry Road
Vicksburg, MS 39180-6199

Final report

Prepared for U.S. Army Corps of Engineers
Washington, DC 20314-1000

ABSTRACT:

For modelers evaluating the impact of dam, levee, and structure failures the need is to be able to determine the flood height and timing. A two-dimensional (2-D) model needs to be able to reproduce this flood wave along the channel and over dry ground. This report details the testing of the 2-D shallow-water module of the ADaptive Hydraulics (ADH) model for surges over initially dry ground. ADH utilizes an unstructured computational mesh that is automatically refined. Other modules in ADH include three-dimensional (3-D) Navier Stokes (with and without the hydrostatic pressure assumption) and groundwater flow. Testing is conducted in comparison to physical flume results for two test cases. The first test case is for a straight flume and the second contains a reservoir and a horseshoe channel section. It is important that the model match the timing of the surge as well as the height. In both cases the ADH compared closely with the flume results.

Contents

List of Figures

Preface

The Civil Works Security and Protection Research and Development Program (CWISP) funded this investigation of the two-dimensional (2-D) shallow-water module of the Adaptive Hydraulics for dam breaks. The Civil Works Security and Protection Research and Development Program was funded by Headquarters, U.S. Army Corps of Engineers (HQUSACE), Office of Homeland Security. Dr. Tony Liu at HQUSACE was the technical monitor and Mr. John Meador was the Headquarters program manager. The U.S. Army Engineer Research and Development Center program manager for CWISP was Dr. Will McMahon of the Geotechnical and Structures Laboratory.

The study was conducted by the Coastal and Hydraulics Laboratory (CHL), U.S. Army Engineer Research and Development Center (ERDC) during the period June 2003 to July 2004. Mr. Thomas W. Richardson, Director, CHL; Dr. W. D. Martin, Deputy Director, CHL; Mr. T. J. Pokrefke, former Chief of Staff, CHL; and Dr. R. T. McAdory, Chief, Tidal Hydraulics Branch, CHL, provided oversight of this project.

This investigation was conducted and the report prepared by Dr. R. C. Berger and Ms. L. M. Lee, both of CHL.

Dr. James R. Houston was Director of ERDC. COL James R. Rowan, EN, was Commander and Executive Director.

1 Introduction

Traditionally, one-dimensional (1-D) hydrodynamic models have been used to predict the impact of dam break, lock failure, levee breach, etc. A 1-D model assumes uniformity in velocity and water-surface elevation over the cross section. Since the actual variation is how energy is removed from the system, a 1-D model will require estimation of energy loss coefficients for expansion and contraction. Generally these coefficients cannot be found by tuning since no similar event in the drainage basin has occurred. The water-surface predictions are sensitive to these coefficients. Two-dimensional (2-D) models represent the lateral as well as the longitudinal variation in velocity and water surface and so are able to reproduce the energy loss with much less uncertainty.

The U.S. Army Corps of Engineers (USACE) needs a 2-D model that will supply hydrodynamic variation laterally and longitudinally in sections with geometric features such as bridges, hydraulic structures, and potential failures. The model should also be able to reproduce levee breach and flooding events with a minimum of coefficient tuning. The purpose of this investigation is to develop a 2-D modeling system that can be rapidly applied to a site and supply accurate hydrodynamic results.

The ADaptive Hydraulics (ADH) model has features that place it as the appropriate code to modify and use for modeling of surges over initially dry land. The primary feature that ADH contains that sets it apart from other codes is in its ability to automatically refine the mesh as demanded by the hydrodynamics. Since dam and levee breaches will not generally allow the user to know ahead of time where resolution will be needed, it is important the model itself can find and refine these areas of hydrodynamic sensitivity. A second important attribute of ADH is that it can run on many platforms from desktop computers to parallel processing supercomputers. The code was designed from the beginning to be a parallel code. If the size of the problem outgrows the desktop computer it can be moved to more powerful computers.

This report begins with a description of the ADH. This includes the manner in which wetting and drying is addressed and is followed by the actual equations that are solved. The next section demonstrates ADH results compared with laboratory results. The final section presents conclusions from the investigation.

2 Model Description

ADH is a finite element code that presently can simulate 3-D unsaturated groundwater flow, 3-D Navier Stokes flow (both hydrostatic and nonhydrostatic), and 2-D shallow-water flow. The code uses linear interpolation for all the variables. ADH uses tetrahedral elements in 3-D and triangle elements in 2-D. ADH is capable of mesh adaptation so that it can automatically split elements to produce a more accurate representation of the hydrodynamics. Later it may recombine elements if the hydrodynamics no longer demands this resolution. This is a tremendous advantage for the user. The modeler need only create a mesh that accurately captures the topography of the domain. The model can then refine the mesh, if necessary, to create an accurate flow field. Without this feature the user would have to either create a highly resolved mesh everywhere, or the user will have to modify the mesh by trial as a run progresses.

ADH uses an inexact Newton technique to develop the linear set of equations from the finite element statement. These algebraic equations are solved for the dependent variables of the shallow-water equations (h,u,v) using the BiCGSTAB algorithm (see Kelley 1995) and a set of preconditioners. The Newton solver is also utilized for wetting-drying problems.

A mesh of smaller segments, called elements, represents the problem domain. The independent variables (x,y) and the dependent variables (h,u,v) are interpolated in each of these elements. The equations of motion and continuity are integrated on combinations of these elements. Portions of the overall domain are going to be dry, and other portions will be wet. One could have elements be either wet or dry, that is, turned on or turned off. However, this on-off switch can result in model instability. It also would require a fine mesh. Instead, ADH integrates the shallow-water equations over the wet portion of an element. A single element that contains the waterline will only partially contribute to the shallow-water equations. In this way the waterline is found indirectly through the iterative process. This adds more nonlinear behavior to the system and is likely to increase the number of nonlinear iterations required for each time-step. However, it allows the model to find the waterline at the same time that the flow variables are calculated.

The following section provides the shallow-water equations as used in ADH.

$$\frac{\partial U}{\partial t}+\frac{\partial F}{\partial x}+\frac{\partial G}{\partial y}+H=0 \tag{1}$$

where

$$U = \begin{pmatrix} h \\ uh \\ vh \end{pmatrix} \tag{2}$$

$$F = \begin{pmatrix} uh \\ u^2h + \frac{1}{2}gh^2 - h\frac{\sigma_{xx}}{\rho} \\ uvh - h\frac{\sigma_{yx}}{\rho} \end{pmatrix} \tag{3}$$

$$G = \begin{pmatrix} vh \\ uvh - h\frac{\sigma_{xy}}{\rho} \\ v^2h + \frac{1}{2}gh^2 - h\frac{\sigma_{yy}}{\rho} \end{pmatrix} \tag{4}$$

and

$$H = \begin{pmatrix} 0 \\ gh\frac{\partial z_b}{\partial x} + \frac{h}{\rho}\frac{\partial P}{\partial x} + \frac{n^2 gu\sqrt{u^2+v^2}}{C_0^2 h^{1/3}} \\ gh\frac{\partial z_b}{\partial y} + \frac{h}{\rho}\frac{\partial P}{\partial y} + \frac{n^2 gv\sqrt{u^2+v^2}}{C_0^2 h^{1/3}} \end{pmatrix} \tag{5}$$

g = acceleration due to gravity

ρ = fluid density

z_b = channel bed elevation

P = pressure at the water surface

n = Manning's roughness coefficient

C_0 = dimensional constant (C_0 = 1 for SI units and C_0 = 1.486 for English units)

The Reynolds stresses are determined using the Boussinesq approach to the gradient in the mean currents:

$$\sigma_{xx} = 2\rho\nu_t \frac{\partial u}{\partial x} \tag{6}$$

$$\sigma_{yy} = 2\rho\nu_t \frac{\partial v}{\partial y} \tag{7}$$

and

$$\sigma_{xy} = \sigma_{yx} = \rho\nu_t \left(\frac{\partial u}{\partial y} + \frac{\partial v}{\partial x}\right) \tag{8}$$

where ν_t = kinematic eddy viscosity (which varies spatially).

The ADH shallow-water equations are placed in conservative form so that mass balance and the balance of momentum and pressure are identical across an interface. This is important in order to match the speed and height of a surge or hydraulic jump.

The equations are represented in a finite element approach. The quality of the numerical solution depends on the choice of basis or trial function and the test function. The trial function determines how the variables are represented and the test function determines the manner in which the differential equation is enforced. In the Galerkin approach the test functions are chosen to be identical with the trial functions. When the flow is advection-dominated, the Galerkin approach produces oscillatory behavior. The basic problem is that the Galerkin form of the test function cannot detect the presence of a node-to-node oscillation and so allows this spurious solution. The approach used in ADH is to enrich the standard Galerkin test function with an additional term that can detect and control this spurious solution.

The Petrov-Galerkin method used here is based on elemental constants for coefficients. This reduces the stabilization to the nonconservative form. This is not a problem since the stabilization is only applied within the elements and uses the Galerkin test function to enforce "flux" balance across element edges. For illustration, consider the shallow-water equations in nonconservative form

$$\frac{\partial U}{\partial t} + A\frac{\partial U}{\partial x} + B\frac{\partial U}{\partial y} + H = 0 \tag{9}$$

where, $A = \frac{\partial F}{\partial U}$; and $B = \frac{\partial G}{\partial U}$. The trial functions (or interpolation/basis functions) are the Lagrange polynomials. These are piecewise linear functions that are continuous across element boundaries. Spatial derivatives, however, are not continuous across these element edges. Each of the dependent and independent variables is interpolated via these trial functions. For example, $\tilde{u}(x) = \sum_{j=1}^{N} \phi_j(x) u_j$, means that the approximate solution, $\tilde{u}(x)$, is made up of the product of the trial function for node j and the nodal value at that location. The test function is chosen as:

$$\varphi_i^* = \phi_i I + \alpha \left(\frac{\partial \phi_i}{\partial x} A + \frac{\partial \phi_i}{\partial y} B \right) \tag{10}$$

where,

$$\alpha = 0.5l \left[\overline{v} \cdot \overline{v} + gh + \left(\frac{l}{\Delta t} \right)^2 \right]^{-1/2} \tag{11}$$

$l = (\Omega_e)^{1/2}$, i.e, the square root of the element area

$\overline{V} = (\overline{u}, \overline{v})$, the element average velocity components

Δt = the time-step size

The finite element statement becomes:

$$\begin{aligned} &\int_{\Omega} \left(\phi_i \frac{\partial U_l}{\partial t} - \frac{\partial \phi_i}{\partial x} F_l - \frac{\partial \phi_i}{\partial y} G_l + \phi_i H_l \right) d\Omega + \\ &\oint_{\partial\Omega} \phi_i \left\{ F_l n_x + G_l n_y \right\} ds + \sum_e \int_{\Omega_e} \alpha \left(\frac{\partial \phi_i}{\partial x} A_l + \frac{\partial \phi_i}{\partial y} B_l \right) \\ &\left(\frac{\partial U_l}{\partial t} + A_l \frac{\partial U_l}{\partial x} + B_l \frac{\partial U_l}{\partial y} + H_l \right) = 0 \end{aligned} \tag{12}$$

where, the subscript l indicates the finite element approximation. The Petrov-Galerkin contributions are integrated on the interior of the elements, but not across element edges. This contribution stabilizes the Galerkin approach. This scheme utilizes a single scaling factor α. This is different from the scheme reported in Berger and Stockstill (1995). That scheme involved scaling each eigenvalue. However, this method does not converge using the iterative solver in ADH. Instead, a single value scaling (Equation 11) is used.

3 Model Tests and Results

A numerical model needs to be produced in a careful manner. The underlying approach must be conservative so that mass and the momentum balance are correctly represented. If not, the speed and location of a shock will be wrong. These comparisons with physical flume results will allow a check on the numerical code. The first case is a straight flume in which a dam is rapidly removed. This produces a surge downstream over initially dry ground and a rarefaction wave moving upstream. The second case also involves an instantaneous dam removal and a surge moving over dry ground. This case includes a curved section of channel. The straight channel is a 1-D problem while the curved channel represents a more general 2-D test case.

Case 1: Straight Flume

The first case is a comparison with results from a study done at ERDC's Waterways Experiment Station (U.S. Army Engineer Waterways Experiment Station 1960; 1961). This study is of a dam break in a straight flume. The flume was 121.9 m (400 ft) in length and had a width of 1.2 m (4 ft). The flume had a slope of 0.0015 m (0.005 ft). The dam is situated 61 m (200 ft) into the flume. Water is pooled upstream of the dam prior to the test. The initial water surface upstream of the dam is flat with the depth at the dam of 0.3048 m (1 ft). Downstream the bed is dry. The water level is recorded at several stations both upstream and downstream of the dam. When the dam is removed, a rarefaction wave propagates upstream and a surge downstream. For this report, the water depth (overland head) at stations 160, 191, 200 (dam), 225, 275, 345 are compared between ADH and the physical model flume. The station numbers indicate the location from the upstream edge of the model. Stations 160 and 191 are upstream of the dam; sta 200 is at the dam location; and stations 225, 275, and 345 are downstream of the dam. Figure 1 shows the initial water surface, the bed, and channel stations.[1]

[1] Figures 1-7 in this report express units of measurement in feet. To convert feet to meters, multiply the number of feet by 0.3048.

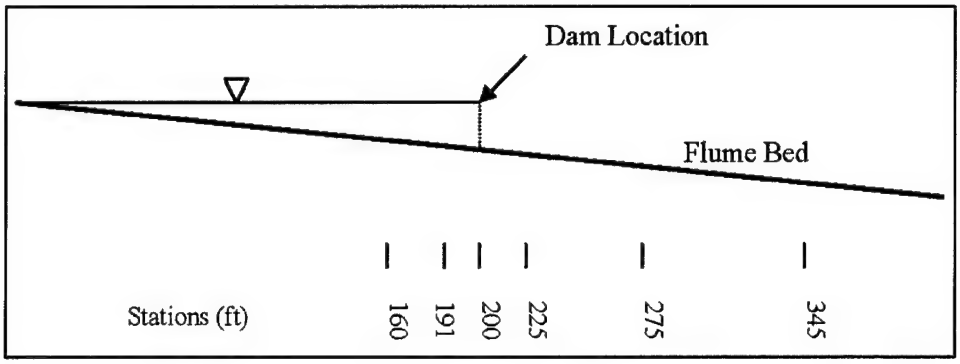

Figure 1. Layout of straight flume, elevation view

The numerical mesh contains 4,000 elements and 2,505 nodes. The downstream model boundary extends 30.5 m (100 ft) beyond that of the flume. This allows the surge to pass out of the model without contaminating the results at the flume stations. The numerical model for this case is treated as a closed region in which the water stays within the domain for the entire run. The upstream and downstream boundaries are treated as impervious wall. Otherwise the numerical flume matched that of the physical flume.

The model parameters are given in Table 1. The Kinematic Eddy Viscosity (EVS) card is used to set the kinematic eddy viscosity and the Molecular Viscosity (MU) card sets the molecular viscosity. The Manning's Roughness Unit Conversion (MUC) card is used for unit conversion with the Manning's roughness formulation. It has a value of 1 for SI units and 1.486 for English units. Density (RHO) and Gravity (G) set the values for density and gravity in the desired units. The Drying Limits (DTL) is used for wetting and drying. The Maximum Levels of Refinement (ML) and Shallow-Water Refinement Tolerance (SRT) card are used for adaptation. The ML card sets the number of times the grid can adapt and the SRT card sets the error level at which the grid will adapt. A value of zero indicates that the same result was obtained with or without adaptation on this particular test case.

Table 1
Test Conditions for Straight Flume Dam Break Case

Condition	Values
Kinematic Eddy Viscosity (EVS)	0.09 0.09 0.09
Molecular Viscosity (MU)	0.0001
Manning's Roughness Unit Conversion (MUC)	1.486
Density (RHO)	1.94
Gravity (G)	32.2
Drying Limits (DTL)	0.01 0.04
Maximum Levels of Refinement (ML)	0
Shallow-Water Refinement Tolerance (SRT)	100
Time-step	0.25
Manning's n	0.009

The time-step is determined by decreasing the size until the results no longer changed. The results are considered converged with a time-step of 0.25 sec. The

physical model study suggests a Manning's n value of 0.009, which is used in the numerical model.

Figures 2 through 7 show the test results for stations 160, 191, 200, 225, 275, and 345. These graphs show a time-history of the water level for both the numerical model and the flume. The arrival time of the wave in ADH agrees with the arrival time from the flume at all stations. Initially the water level in the model seems to fall at the same rate as in the flume for both the upstream stations. Near the end of the run, the water level in the flume drops off more rapidly than predicted in the model (see Figures 2 and 3). The flume results at the site of the dam, sta 200, show a surge superimposed on the overall water-surface drop. The numerical model captures the overall drop but not the superimposed surge. The maximum difference at this station occurs at a time of 50 sec.

The three downstream stations (225, 275, and 345), shown in Figures 5, 6, and 7, also have some points that differ from the physical model by as much as 0.04. Overall the water level predicted by the numerical model is in close agreement with the data from the flume. At sta 225 (Figure 5) the time of arrival of the water-surface peak predicated in the numerical model agrees with that of the flume although there is a 3 percent error in the maximum water level. The time predicted for maximum water level at sta 275 (Figure 6) is 5 sec earlier than seen in the flume. This is about a 14 percent error. The peak elevation at this station also differs by 11 percent from the flume. The last station, 345 (Figure 7), has only a 5 percent error in the maximum water level and the predicted time agrees with the flume. The rise in the water level in the numerical model after 125 sec is due to the water collecting above the lower boundary of the numerical model. This is after the time of comparison to the physical flume.

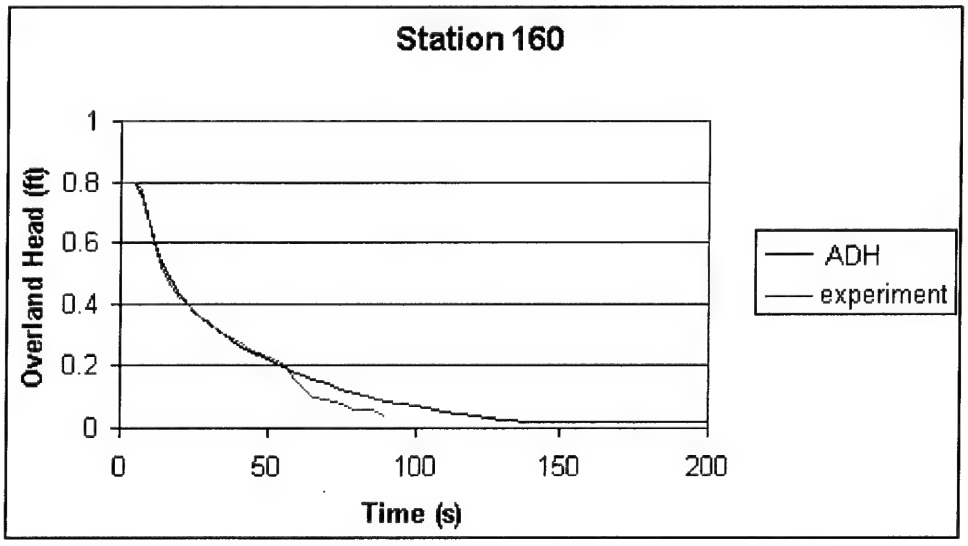

Figure 2. Depth comparison for ADH and flume experiment, sta 160

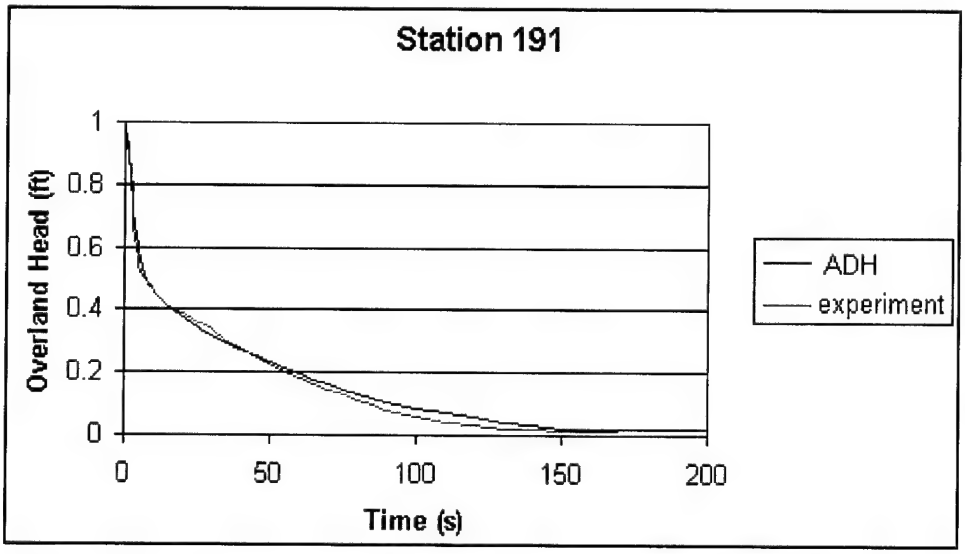

Figure 3. Depth comparison for ADH and flume experiment, sta 191

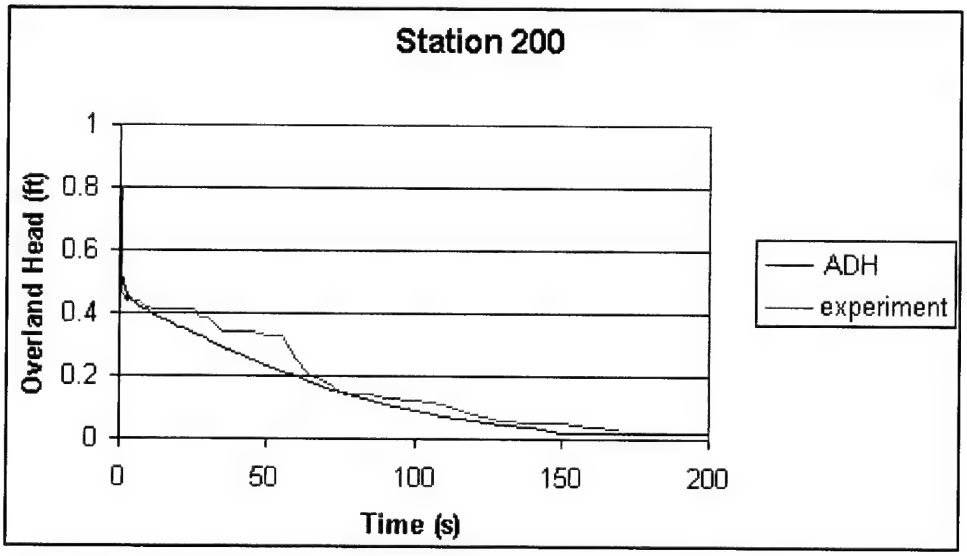

Figure 4. Depth comparison for ADH and flume experiment, sta 200

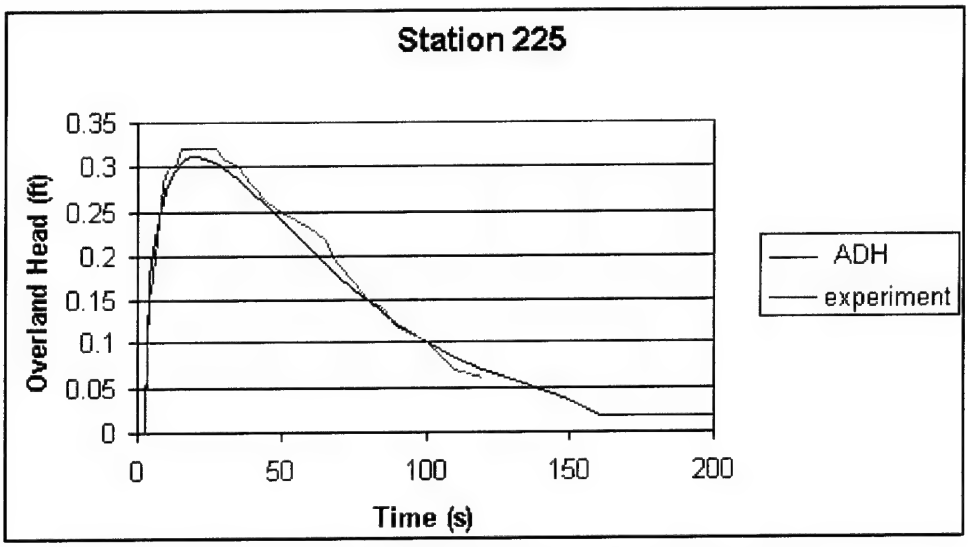

Figure 5. Depth comparison for ADH and flume experiment, sta 225

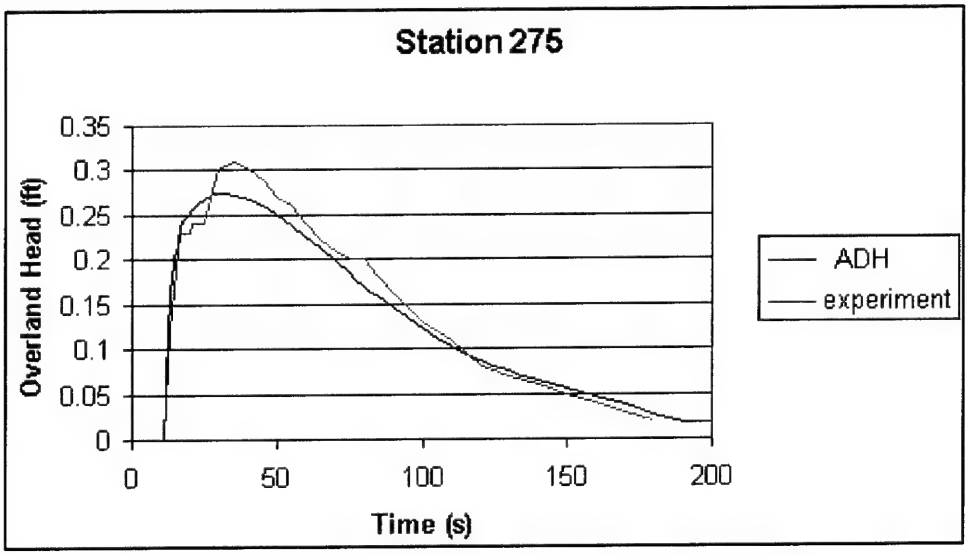

Figure 6. Depth comparison for ADH and flume experiment, sta 275

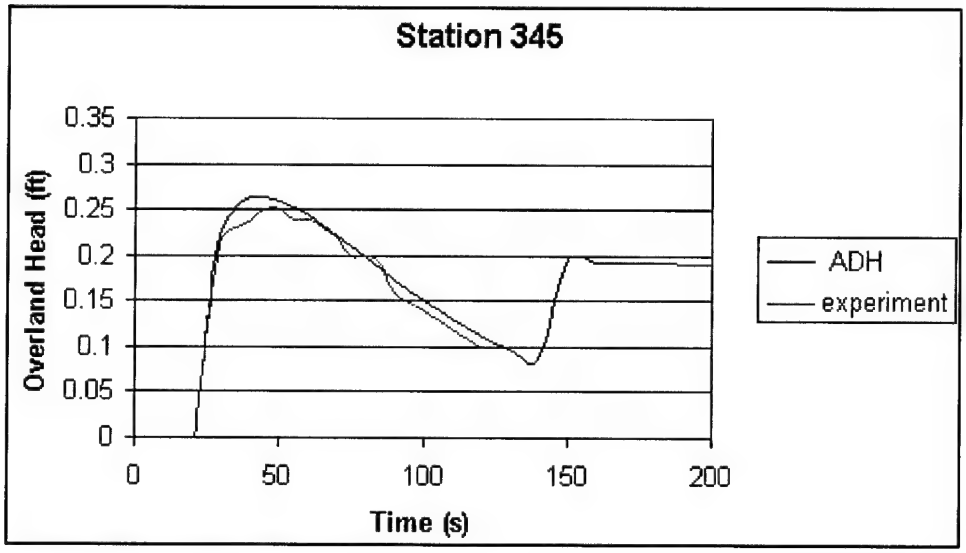

Figure 7. Depth comparison for ADH and flume experiment, sta 345

Case 2: Horseshoe Curve Flume

The second case is a comparison with a study done by Bell et al. (1992). Figure 8 shows a plan view of the flume used in the study. The flume is composed of a reservoir section and a channel section. The reservoir has a bottom elevation of 0.089 m (0.291 ft) lower than the channel bed. The initial water depth in the reservoir is 0.305 m (1 ft) and the channel is dry. The water is pooled in the reservoir. The water level in the flume and the time was recorded at five of the eight stations. No data were provided at stations 3, 5, and 7 from the flume study. Sta 1 is located in the straight channel section 0.3 m (1 ft) downstream from the dam. Stations 2, 4, and 6 are in the curved section of the flume. Sta 2 is 3 deg into the curve; sta 4 is 90 deg into the curve; and sta 6 is 177 deg into the curve. Sta 8 is located 2.29 m (7.51 ft) from the end of the curve. The numerical model parameters are given in Table 2.

Table 2
Test Conditions for Horseshoe Curve Flume Dam Break Case

Condition	Values
EVS	0.008 0.008 0.008
MU	0.00001
MUC	1
RHO	1000
G	9.81
DTL	0.004 0.01
ML	2
SRT	3
Time-step	0.03
Manning's n	0.009

The grid used in the numerical model is shown in Figure 9. This initial grid has 899 elements and 532 nodes. ADH automatically refines the mesh based upon the hydrodynamic error measured during the simulation so the initial grid is the smallest number of elements and nodes for the model test. The Bell et al. (1992) article suggests a Manning's n value of 0.0165 based on their numerical model study. However, prior experience suggests this is far too high for a Plexiglas flume. Instead a Manning's n value of 0.009 is used, which is consistent with other studies done in smooth flumes, e.g., Berger (1993); Berger and Stockstill (1995); and Stockstill et al. (1997); and the straight channel test in this report. A Manning's n value of 0.009 is in line with the recommended values found in Chow (1959) and Henderson (1966).

The test result comparisons are shown in Figures 10 through 14. In these graphs, symbols indicate the experimental data and a solid line indicates the numerical data. The outer wave is shown in blue and the inner wave in red. At stations 1, 6, and 8 (Figures 10, 13, and 14, respectively) the predicted arrival time from the numerical model agrees with the time observed in the flume. The predicted arrival time at sta 2 (Figure 11) is approximately one tenth of a second early, which is about a 1 percent error. The predicted arrival time for the inner wave at sta 4 (Figure 12) is early by three tenths of a second (a 4 percent error) and the outer wave is early by two tenths of a second (a 6 percent error). All of these arrival times are likely within the test uncertainty in the physical flume. The predicted water level rises at the same rate seen in the flume at stations 1, 2, and 8. At sta 4 the predicted water level rises at a rate that is a bit slower than seen in the flume for the outer wall, but along the inner wall the water level increases at the same rate. The difference between the inside and the outside wall water-surface elevations is small. At sta 6 the water level along the outer wall rises at the same rate, but along the inner wall the water level rises more slowly than seen in the flume. The predicted maximum height agrees with the water levels seen in the flume at all stations except sta 2. In the results from the flume, the maximum water-level record at this location is around 0.043 m (0.141 ft). At the time these maximum heights are observed in the flume, the numerical model predicts a height of 0.067 m (0.219 ft) and by the end of the run the numerical model has a height of 0.09 m (0.29 ft).

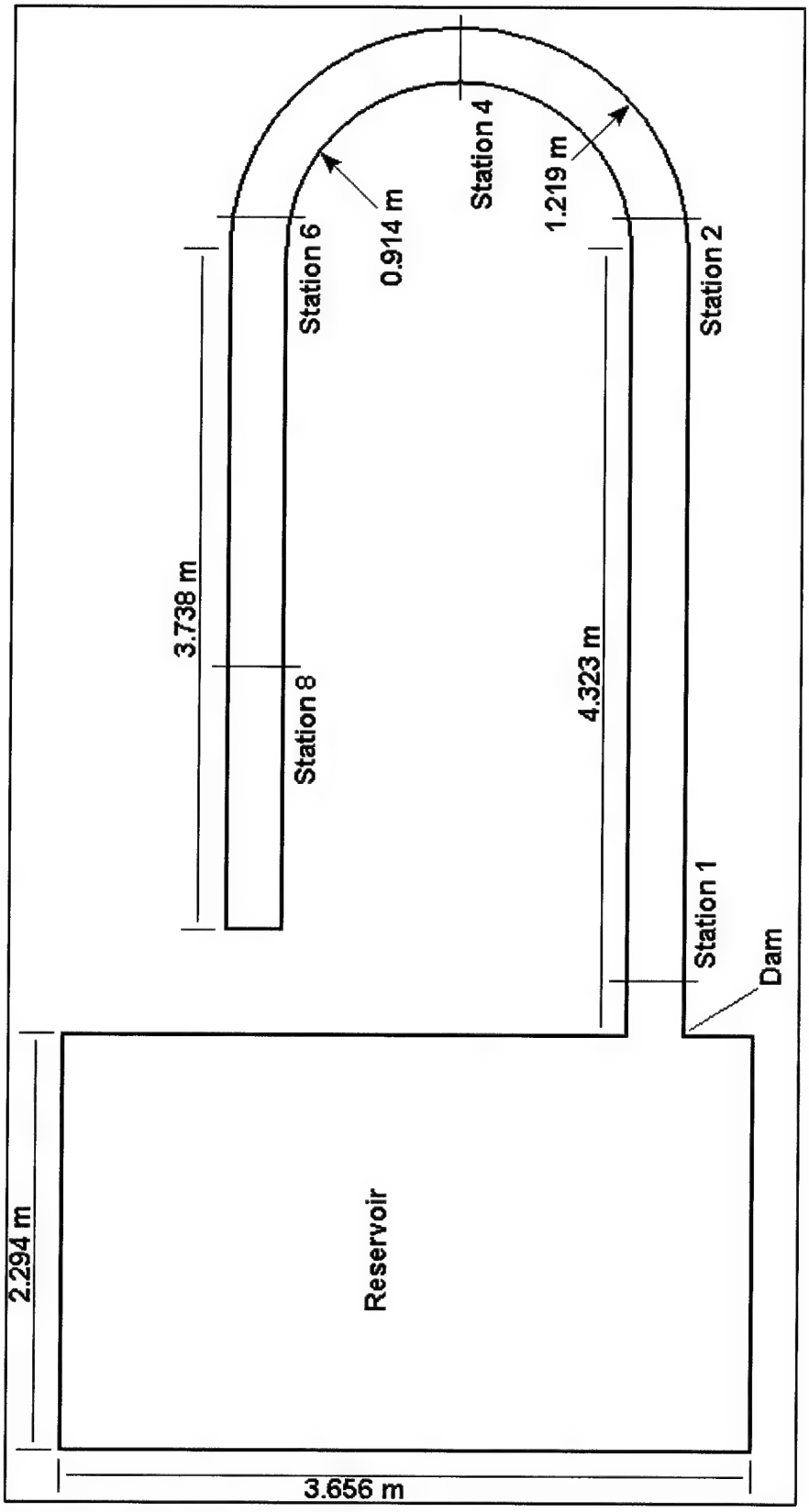

Figure 8. Plan view of flume

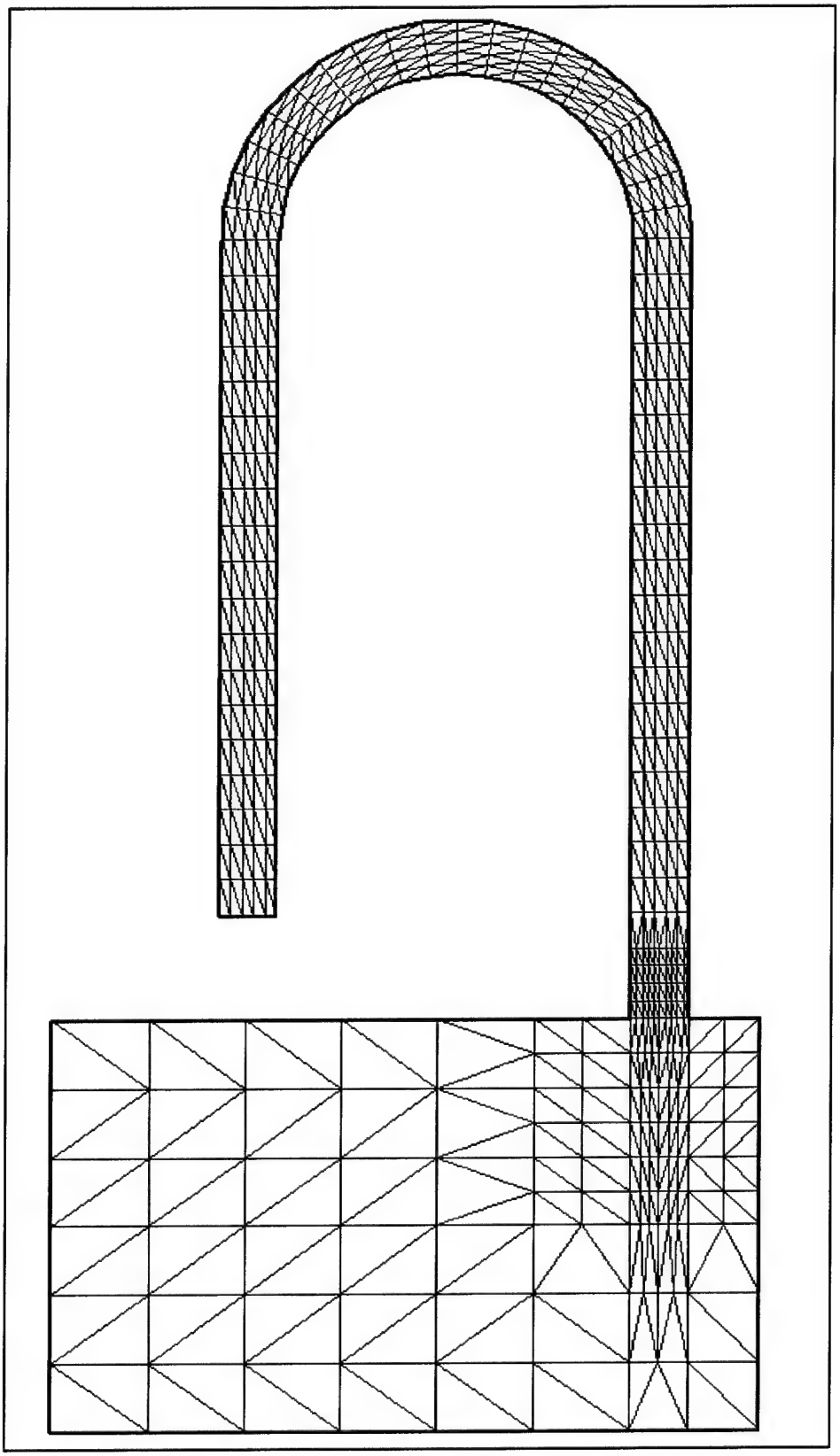

Figure 9. Initial grid for ADH

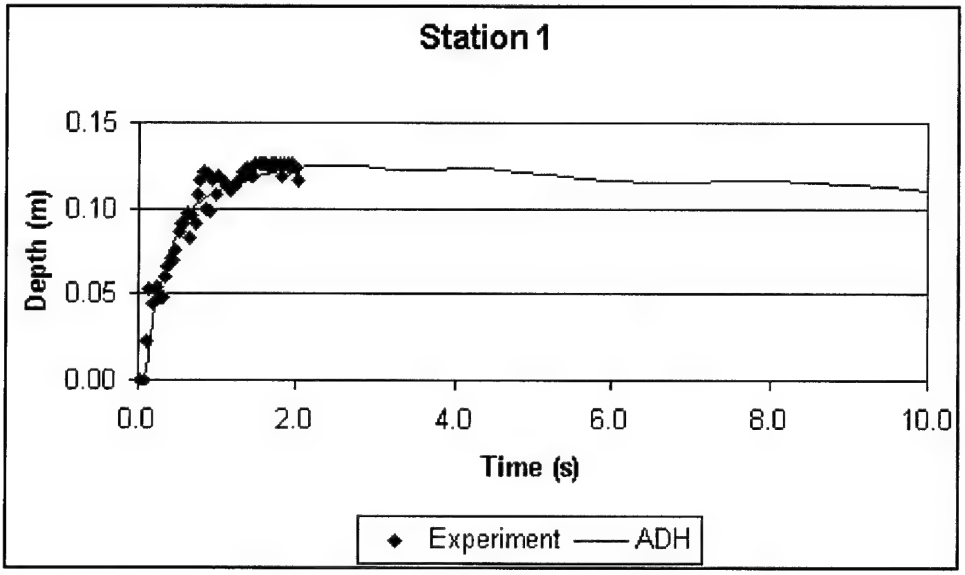

Figure 10. Depth comparison for ADH and flume experiment, sta 1

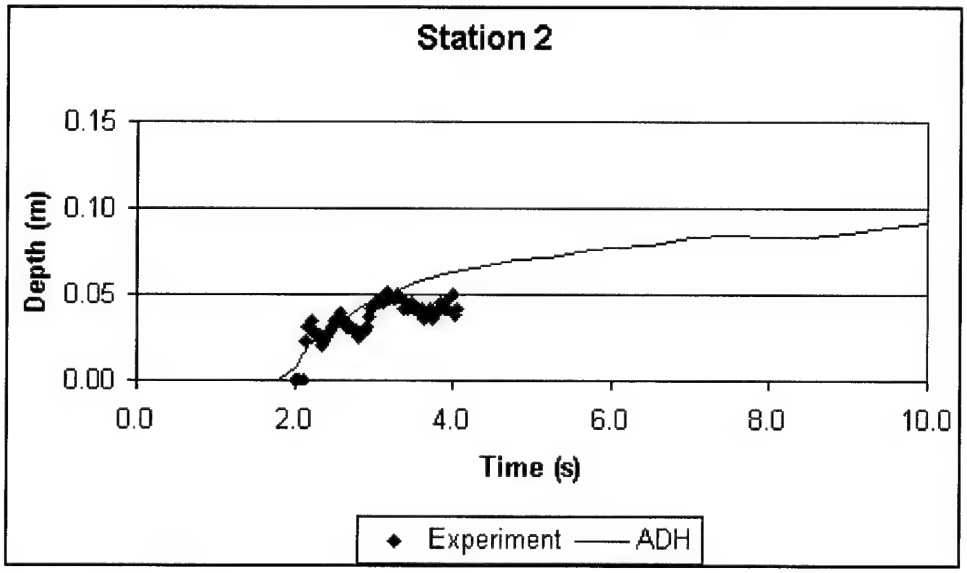

Figure 11. Depth comparison for ADH and flume experiment, sta 2

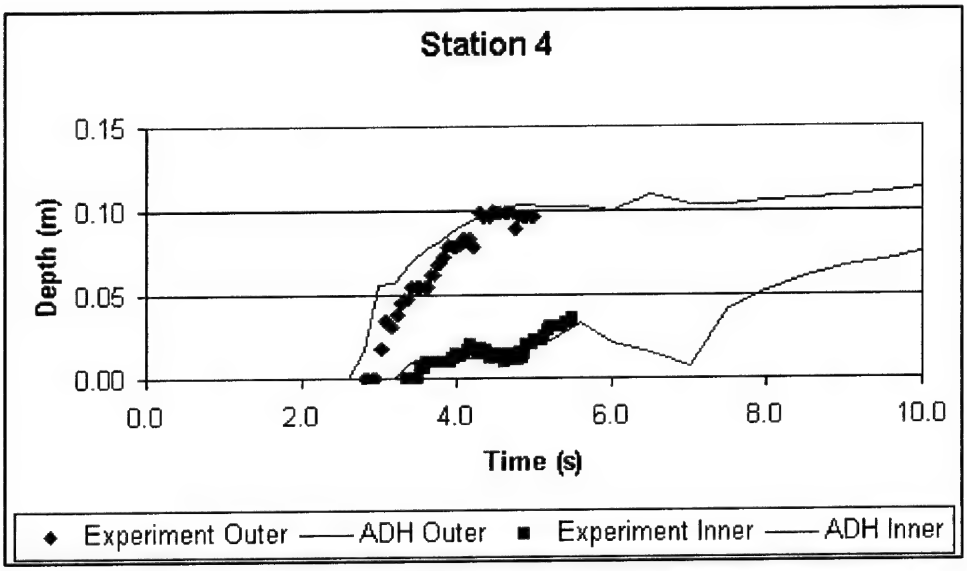

Figure 12. Depth comparison for ADH and flume experiment, sta 4

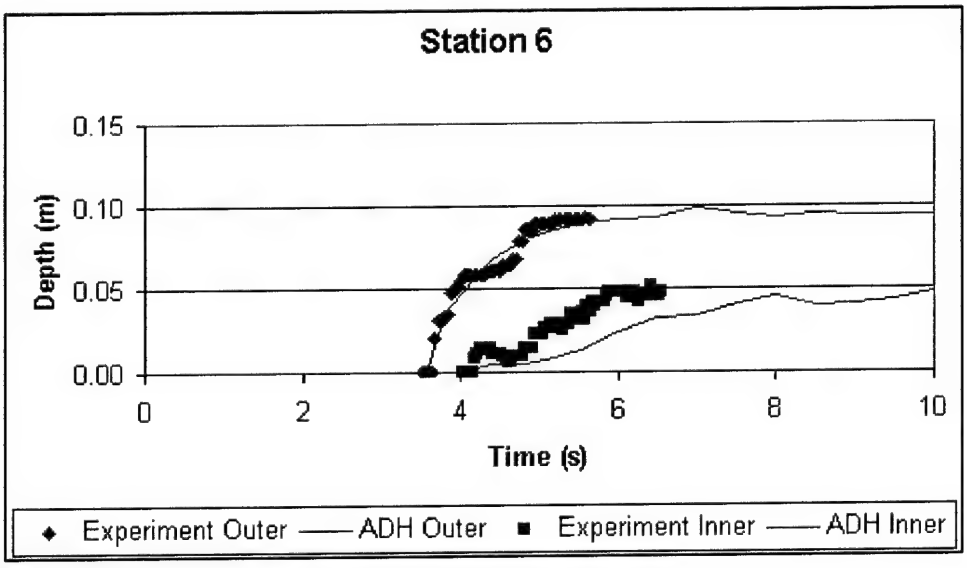

Figure 13. Depth comparison for ADH and flume experiment, sta 6

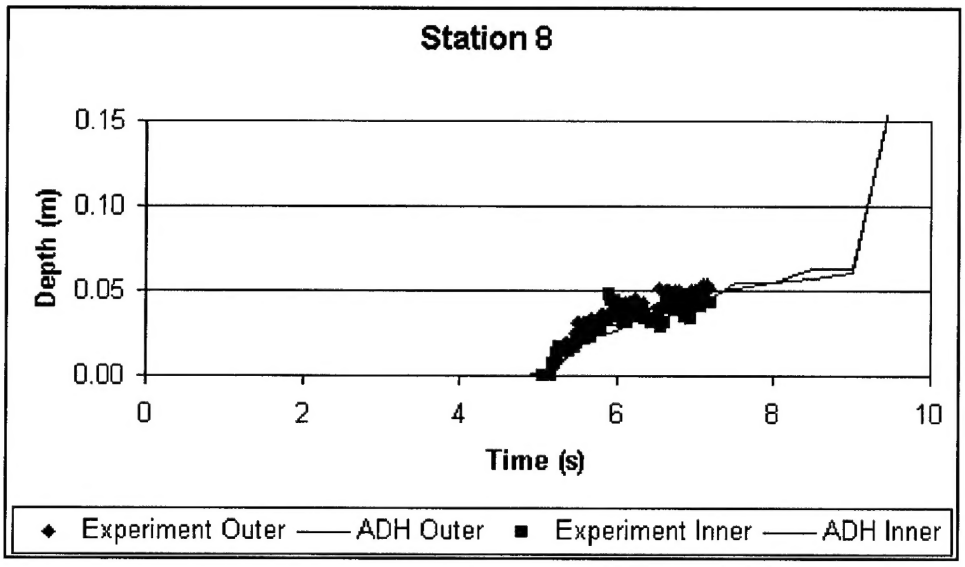

Figure 14. Depth comparison for ADH and flume experiment, sta 8

4 Conclusions

One of the key characteristics for this type of problem that ADH must reproduce is the timing of the surge. If the formulation is not fully conservative, the speed of the surge will not match. There are six comparison locations in test 1 and eight locations in test 2. Overall the two test cases show ADH matches the surge speed very well at all stations.

The other key characteristic is the height of the surge. Of the six data locations in test 1, five of the six closely match. In the eight data locations in test 2, six compare closely. ADH matches surge heights well.

Parameters are selected based upon reasonably well known values. The model comparisons are accomplished without need for tuning. This investigation shows that ADH compares well with tests of dam break and surge propagation.

References

Bell, S. W., Elliot, R. C., and Chaudhry, M. H. (1992). "Experimental results of two-dimensional dam-break flows," *Journal of Hydraulic Research* 30(2), 225-252.

Berger, R. C. (1993). "A finite element scheme for shock capturing," Technical Report TR-93-12, U.S. Army Engineer Waterways Experiment Station, Vicksburg, MS.

Berger, R. C., and Stockstill, R. L. (1995). "Finite element model for high-velocity channels." *Journal of Hydraulic Engineering* ASCE, 121(10), 710-716.

Chow, V. T. (1959). *Open-channel hydraulics*. McGraw-Hill, Inc., 110.

Henderson, F. M. (1966). *Open channel flow*. The Macmillan Co., New York, 99.

Kelley, C. T. (1995). *Iterative methods for linear and nonlinear equations*. Frontiers in Applied Mathematics, Vol. 16, Society for Industrial and Applied Mathematics, Philadelphia, PA.

Stockstill, R. L., Berger, R. C., and Nece, R. E. (1997). "Two-dimensional flow model for trapezoidal high-velocity channels," *Journal of Hydraulic Engineering* ASCE, 123(10), 844-852.

U.S. Army Engineer Waterways Experiment Station. (1960). "Floods resulting from suddenly breached dams: Conditions of minimum resistance," Miscellaneous Paper No. 2-374, Report 1, Vicksburg, MS.

U.S. Army Engineer Waterways Experiment Station. (1961). "Floods resulting from suddenly breached dams: Conditions of high resistance," Miscellaneous Paper No. 2-374, Report 2, Vicksburg, MS.

REPORT DOCUMENTATION PAGE

Form Approved
OMB No. 0704-0188

1. REPORT DATE *(DD-MM-YYYY)*	2. REPORT TYPE	3. DATES COVERED *(From - To)*
September 2004	Final report	

4. TITLE AND SUBTITLE

Multidimensional Numerical Modeling of Surges Over Initially Dry Land

5a. CONTRACT NUMBER

5b. GRANT NUMBER

5c. PROGRAM ELEMENT NUMBER

6. AUTHOR(S)

R. C. Berger, L. M. Lee

5d. PROJECT NUMBER

5e. TASK NUMBER

5f. WORK UNIT NUMBER

7. PERFORMING ORGANIZATION NAME(S) AND ADDRESS(ES)

U.S. Army Engineer Research and Development Center
Coastal and Hydraulics Laboratory
3909 Halls Ferry Road, Vicksburg, MS 39180-6199

8. PERFORMING ORGANIZATION REPORT NUMBER

ERDC/CHL TR-04-10

9. SPONSORING / MONITORING AGENCY NAME(S) AND ADDRESS(ES)

U.S. Army Corps of Engineers
Washington, DC 20314-1000

10. SPONSOR/MONITOR'S ACRONYM(S)

11. SPONSOR/MONITOR'S REPORT NUMBER(S)

12. DISTRIBUTION / AVAILABILITY STATEMENT

Approved for public release; distribution is unlimited.

13. SUPPLEMENTARY NOTES

14. ABSTRACT

For modelers evaluating the impact of dam, levee, and structure failures the need is to be able to determine the flood height and timing. A two-dimensional (2-D) model needs to be able to reproduce this flood wave along the channel and over dry ground. This report details the testing of the 2-D shallow-water module of the ADaptive Hydraulics (ADH) model for surges over initially dry ground. ADH utilizes an unstructured computational mesh that is automatically refined. Other modules in ADH include three-dimensional (3-D) Navier Stokes (with and without the hydrostatic pressure assumption) and groundwater flow. Testing is conducted in comparison to physical flume results for two test cases. The first test case is for a straight flume and the second contains a reservoir and a horseshoe channel section. It is important that the model match the timing of the surge as well as the height. In both cases the ADH compared closely with the flume results.

15. SUBJECT TERMS

Two-dimensional
Finite element
Flooding
Flume
Surge

16. SECURITY CLASSIFICATION OF:			17. LIMITATION OF ABSTRACT	18. NUMBER OF PAGES	19a. NAME OF RESPONSIBLE PERSON
a. REPORT	b. ABSTRACT	c. THIS PAGE			19b. TELEPHONE NUMBER *(include area code)*
UNCLASSIFIED	UNCLASSIFIED	UNCLASSIFIED		26	